

Enzyme-Responsive Multifunctional Magnetic Nanoparticles for Tumor Intracellular Drug Delivery and Imaging

Yanmei Yang,^[a] Junxin Aw,^[a] Kai Chen,^[b] Fang Liu,^[a] Parasuraman Padmanabhan,^[c] Yanglong Hou,^[d] Zhen Cheng,^{*,[b]} and Bengang Xing^{*,[a]}

Abstract: Enzyme-responsive, hybrid, magnetic silica nanoparticles have been employed for multifunctional applications in selective drug delivery and intracellular tumor imaging. In this study, doxorubicin (Dox)-conjugated, enzyme-cleavable peptide precursors were covalently tethered onto the surface of uniform silica-coated magnetic

nanoparticles through click chemistry. This enzyme-responsive nanoparticle conjugate demonstrated highly efficient Dox release upon specific enzyme in-

teractions in vitro. It also exhibits multiple functions in selective tumor intracellular drug delivery and imaging in the tumor cells with high cathepsin B expression, whereas it exhibited lower cytotoxicity towards other cells without enzyme expression.

Keywords: click chemistry • doxorubicin • drug delivery • enzymes • intracellular imaging

Introduction

Multifunctional nanoparticles and their potential biomedical applications in therapy and diagnosis have received considerable attention.^[1] Among various colloidal nanostructured materials, superparamagnetic iron oxide nanoparticles (Fe-

NPs) have been of great interest owing to their easy preparation, biocompatibility, and magnetic properties.^[1,2] Currently, Fe-NPs have been extensively employed in cell targeting, bioseparation, and magnetic resonance imaging (MRI) in vitro and in vivo.^[1c,d,3] Tremendous efforts have also been conducted to broaden the applications of these nanoparticles for the controlled delivery of antitumor drugs.^[4,5] For example, the immobilization of Fe-NPs on mesoporous silica nanoparticles has been developed and the surface adsorption of anticancer drugs in the prepared silica-Fe-NP complex supplied a unique platform to achieve MRI detection and deliver drugs to the tumors.^[4b,e] Similarly, the incorporation of anticancer drug and magnetic nanoparticles within polymer or micelle structures has also been investigated to efficiently perform magnetically guided drug release and effective tumor imaging in vitro and in vivo.^[5] However, despite significant success in molecular imaging and drug delivery, the release of drug moieties from these complexed silica magnetic or magneto-polymeric nanohybrids was normally achieved through a passive diffusion mechanism that could potentially undermine the targeting efficiency and specificity of the nano-bioconjugates in the living system. The development of a simple, stable, and covalently conjugated drug-nanoparticle hybrid system that would allow more selective drug release into targeted locations upon specific biological stimuli and meanwhile would also enable the real-time monitoring of drug delivery at the single cell level is still highly desirable and remains a challenge in the field.

[a] Y. Yang, J. Aw, F. Liu, Prof. Dr. B. Xing
Division of Chemistry and Biological Chemistry
School of Physical and Mathematical Sciences
Nanyang Technological University
Singapore 637371 (Singapore)
Fax: (+65) 6791-1961
E-mail: Bengang@ntu.edu.sg

[b] K. Chen, Prof. Dr. Z. Cheng
Molecular Imaging Program at Stanford (MIPS)
Department of Radiology
Stanford University Medical Center
California, 94305 (USA)
E-mail: Zcheng@stanford.edu

[c] Dr. P. Padmanabhan
Translation Molecular Imaging Group (TMIG), Singapore
Bio-Imaging Consortium (SBIC), A*Star
Singapore 138667 (Singapore)

[d] Prof. Dr. Y. Hou
Department of Advanced Materials and Nanotechnology
College of Engineering
Peking University
Beijing 100871 (China)

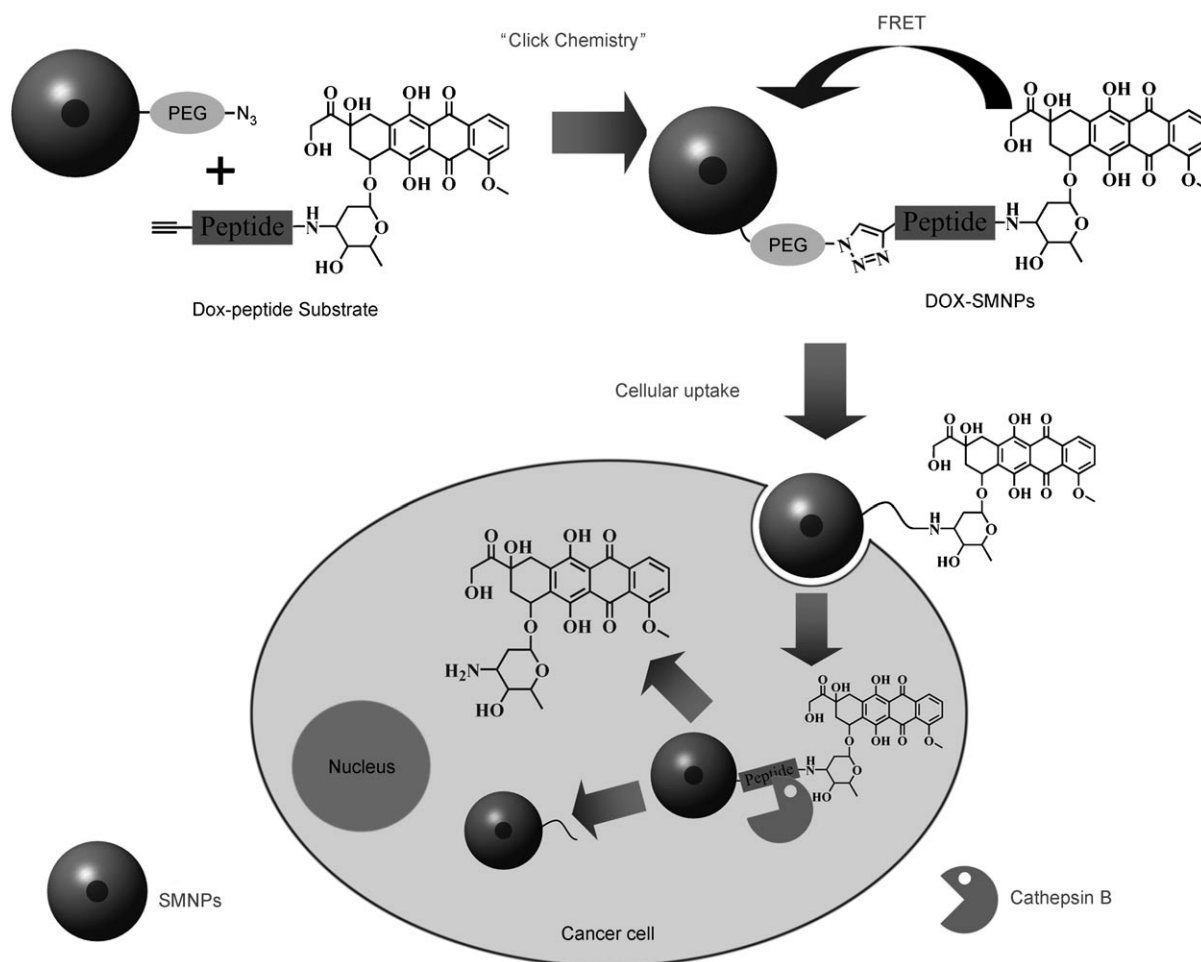
Supporting information for this article is available on the WWW under <http://dx.doi.org/10.1002/asia.201000905>.

Herein, we present the rational design and development of a novel enzyme-responsive, doxorubicin (Dox)-peptide coated, magnetic silica nanoparticle (SMNP) conjugate for selectively triggered intracellular delivery of Dox, which is a commonly used lipophilic antitumor drug, into the tumor cells with specific protease enzyme expression. This nanoparticle conjugate also provides the opportunity to monitor the cellular trafficking of Dox molecules under the living conditions in real time by a combination of MRI and fluorescence imaging techniques.

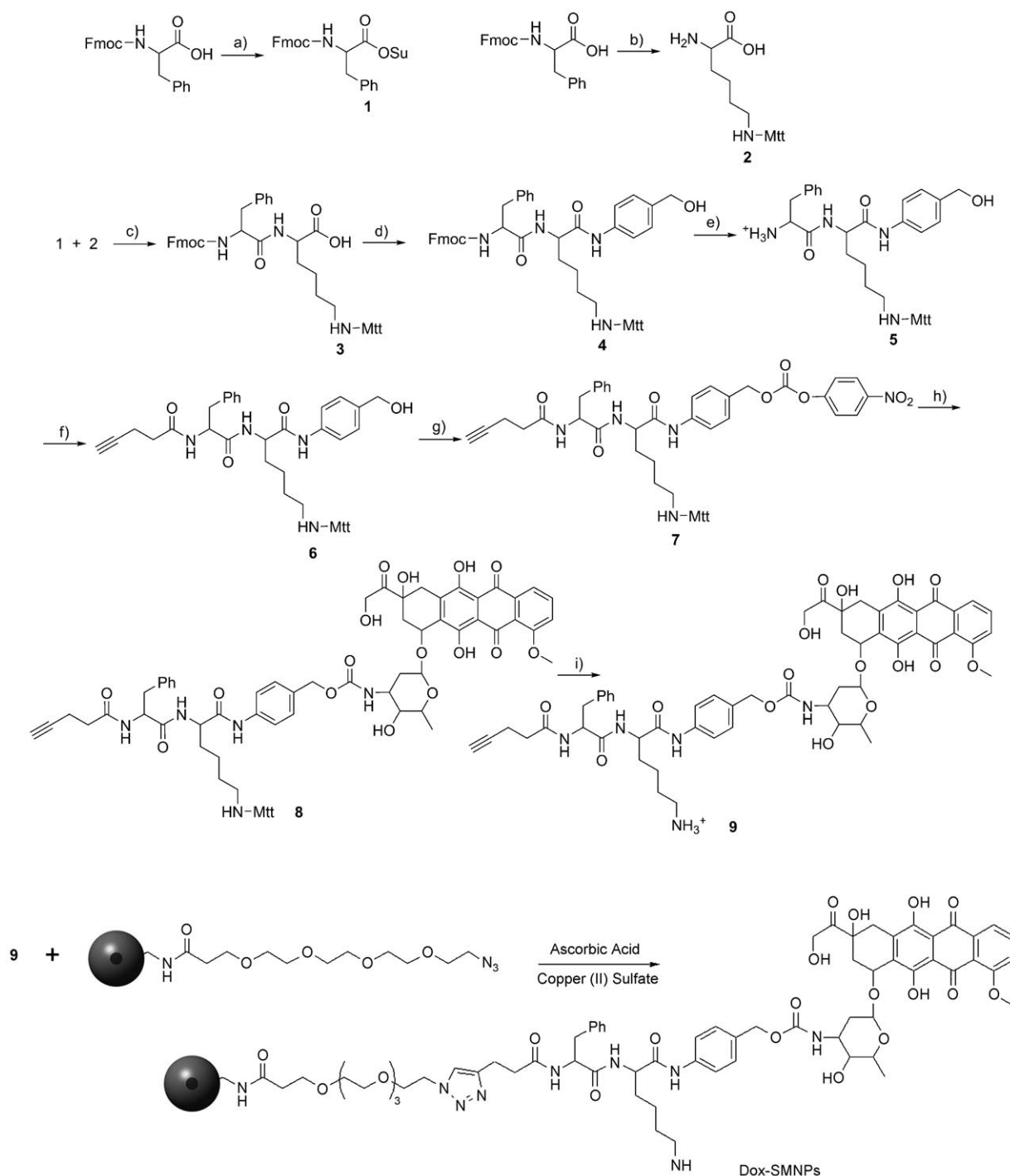
Results and Discussion

As a proof of concept, we designed a uniform silica-coated magnetic nanoparticle (SMNP) complex, which was tethered to a Dox-peptide substrate moiety. The Dox-peptide prodrug was synthesized by coupling the anticancer drug Dox with a peptide sequence H-Phe-Lys-OH under solution-phase conditions (Scheme 1). A self-immolative *para*-aminobenzyloxycarbonyl (PABC) linker was required to combine Dox with the dipeptide sequence. Typically, the dipeptide

sequence of H-Phe-Lys-OH can be selectively recognized and cleaved by cathepsin B, which is a ubiquitous intracellular cysteine protease overexpressed in a variety of malignant tumors,^[6] and is applied as an important target for tumor cell imaging and prodrug development.^[7] Upon cathepsin B enzyme cleavage, an *p*-aminobenzyloxycarbonyl-Dox (PABC-Dox) intermediate is exposed from the Dox-peptide substrate. The Dox-peptide then undergoes 1,6-elimination and decarboxylation to hydrolytically decompose the immolative PABC linker, and therefore, release free Dox antitumor from the Dox-peptide conjugate (Scheme 2). This enzyme-responsive drug release was further confirmed by HPLC analysis (Figure S1 in the Supporting Information). The incubation of Dox-peptide substrate with cathepsin B resulted in efficient enzyme cleavage over a period of five hours. At 485 nm, the peak at 18.2 minutes that corresponded to the Dox-peptide substrate significantly decreased in the presence of enzyme for 5 hours, meanwhile, a new enzymatic product peak with a retention time of 13.9 minutes increased accordingly, which corresponded to the free Dox drug molecule. The chromatographic results clearly indicated that it was the enzyme-mediated reaction that led to the



Scheme 1. Schematic illustration of synthesis of Dox SMNPs and their cellular functions for drug release and tumor imaging. FRET=fluorescence resonant energy transfer.



Scheme 2. Synthesis of the Dox SMNP substrate. a) *N*-Hydroxylsuccinimide (HOSu), 1-ethyl-3-(3-dimethylaminopropyl)carbodiimide (EDC), tetrahydrofuran (THF), 0°C to RT; b) piperidine, *N,N*-dimethylformamide (DMF), RT; c) Et₃N, THF/DMF, RT; d) *p*-aminobenzyl alcohol (PABOH), 2-ethoxy-1-ethoxycarbonyl-1,2-dihydroquinoline (EEDQ), CH₂Cl₂, RT; e) diethylamine, CH₂Cl₂, RT; f) 4-pentynoic acid, HOSu, EDC; Et₃N, THF, 0°C; g) bis(*p*-nitrophenyl) carbonate (bis-PNP carbonate), *N,N*-diisopropylethylamine (DIPEA); h) Dox-HCl, Et₃N, DMF, RT; i) 0.5% trifluoroacetic acid (TFA), CH₂Cl₂, 0°C. Fmoc = fluorenylmethyloxycarbonyl, Mtt = 4-methyltrityl.

effective release of free drug from the Dox-peptide substrate.

The silica magnetic nanoparticle complex was synthesized by the Stöber method.^[8] Hydrophilic iron oxide particles were first prepared in an aqueous phase. Silane-containing

amine functional groups were then used to coat the iron oxide particles to form core-shell magnetic silica structures. This core-shell silicon-coated structure exhibited the advantages of stabilizing the nanoparticle suspension in biological systems and enabling easy surface modification for further

practical applications.^[4b,9] To achieve effective peptide prodrug loading onto the surface of the as-prepared nanoparticles and also to improve the dispersion stability of drug-coated nanoparticles in aqueous solution, the Dox-peptide was modified with an alkynyl group and an azido oligo-(ethylene)glycol (azido-dPEG₄) linker was coupled to the silica-coated magnetic nanoparticles.^[4a,b,10] The alkynyl-peptide prodrug can efficiently conjugate with azido-dPEG₄-modified nanoparticles through [2+3] cycloaddition to produce uniformly drug-loaded functional SMNPs (Scheme 1). The loading amount of Dox-peptide substrate on the surface of the SMNPs was determined by the difference in UV absorbance spectra (Figure S2 in the Supporting Information) and the optimal drug-loading content of Dox to SMNPs was about 5%, which was comparable with the results reported previously.^[4b,c,5a] The hydrodynamic diameter and size distribution of the prodrug-conjugated SMNPs were then characterized by laser dynamic light scattering (DLS) and transmission electron microscopy (TEM). The results indicated the narrow size distribution of the prodrug-conjugated SMNPs with an overall diameter of 50 nm (Figure 1a), which would be the most suitable size to achieve ef-

fective cell penetration.^[1c,11] The magnetic property of the Dox-conjugated SMNPs was verified by measuring transverse (T₂) relaxation times of dispersed nanoparticles on a MRI equipment at 7.0 T. T₂-weighted MRI results indicated the significant signal changes at various concentrations of particles. The specific relaxivity value (r_2) was calculated to be 136 mm⁻¹s⁻¹, which is close to the value determined by using the commercially available Fe₃O₄ nanocrystal Feridex (142 mm⁻¹s⁻¹) (Figure 1b). Moreover, this Dox-coated SMNP (Dox-SMNP) conjugate exhibited good biocompatibility and was stable in buffer solution for more than one month without any changes; this enabled the Dox-SMNP conjugates to be used as a stable and effective contrast agent for subsequent multifunctional applications in targeted drug delivery and intracellular tumor imaging.

The activity of Dox-SMNPs towards enzyme reactions was examined through detecting the fluorescence of Dox. Briefly, free Dox exhibited a fluorescence emission at 590 nm with an excitation at 485 nm. The fluorescence of Dox would be quenched when the drug-modified peptide sequence was covalently tethered on the surface of SMNPs as a result of electronic energy transfer.^[5a] As expected, upon the incubation of Dox-SMNPs with protease cathepsin B at 37 °C in acetic buffer solution (pH 5.0), sequential fluorescent enhancement in the intensity of the native spectrum of Dox was observed, which corresponded to the release of drug molecules from Dox-SMNPs and approximately 80% of the free drug could be released within 6 hours (Figure 2a). Drug release was also monitored in the buffer solution without enzyme treatment and there was no significant fluorescent enhancement observed, indicating good stability and minimal nonspecific drug release from Dox-SMNP conjugates (Figure 2a). Similar drug release measurements were also conducted in the presence of a potent cathepsin B inhibitor, antipain hydrochloride. The enzyme activity decreased dramatically and only limited fluorescence enhancement could be detected, as shown in Figure 2b, which clearly demonstrates effective Dox release from Dox-SMNPs upon specific cathepsin B enzyme interactions.

The intracellular uptake and distribution of the drug-conjugated SMNP complex was monitored by a fluorescent imaging technique. In this study, the cancer cell line HT-29, which highly expresses protease cathepsin B, was chosen as a positive target cell line.^[7b] As a negative control, NIH/3T3 cells were used, since there was no cathepsin B expression in this cell line. Typically, both HT-29 and NIH/3T3 cells were cultured and incubated with 5.0 μM drug-conjugated SMNPs in Dulbecco's modified eagle medium (DMEM) at 37 °C for 2 h to obtain an effective live cell fluorescent imaging. After incubation for two hours, a bright red fluorescence signal was observed mainly in the cytoplasm and not in the cell nuclei of HT-29 cells (Figure 3b), probably owing to the involvement of endocytosis during the uptake of Dox-SMNPs.^[4,12] In contrast, there was no clear fluorescence detected in NIH/3T3 cells (Figure 3a) and HT-29 cells pretreated with the cathepsin B enzyme inhibitor antipain hydrochloride (Figure 3c and Figure S3 in the Supporting

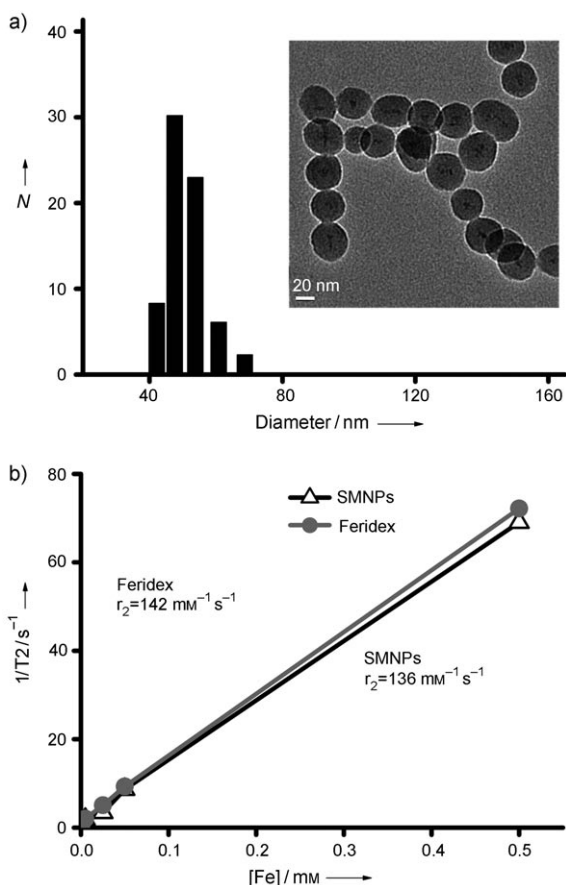


Figure 1. Characterization of synthesized SMNPs. a) The size distribution of SMNPs determined by DLS and TEM imaging (inset, scale bar = 20 nm). b) The specific relativity value (r_2) of SMNP (Δ ; $r_2 = 136 \text{ mm}^{-1} \text{ s}^{-1}$) and commercially available Feridex (\bullet ; $r_2 = 142 \text{ mm}^{-1} \text{ s}^{-1}$) nanoparticles.

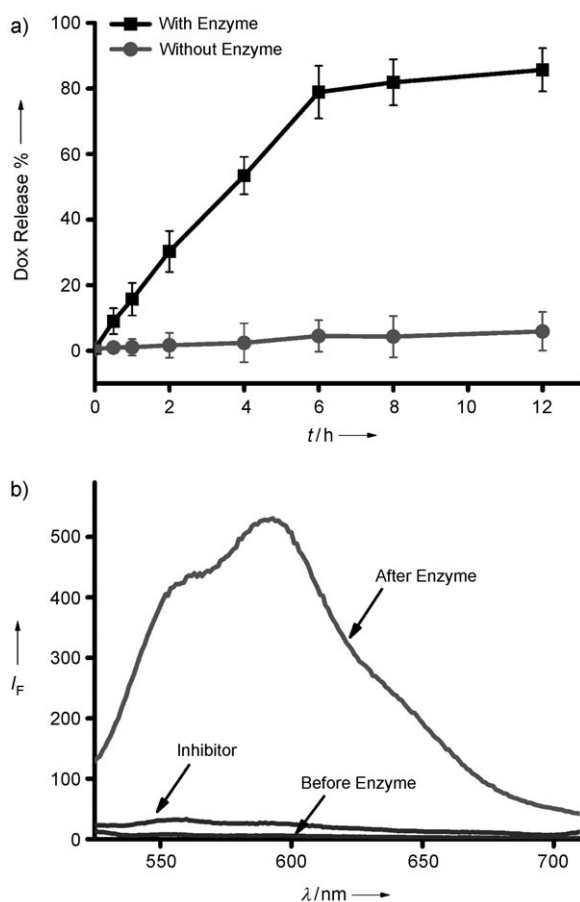


Figure 2. a) Dox release upon cathepsin B (33 nM) enzymatic reaction with Dox-SMNPs (100 μ M) at different times (0–6.0 h) ($\lambda_{\text{ex}}=485$ nm, $\lambda_{\text{em}}=590$ nm). b) Fluorescence enhancement of Dox-SMNPs when treated with cathepsin B in the absence and presence of the enzyme inhibitor antipain hydrochloride.

Information). The results clearly indicated that Dox-SMNPs could easily enter into the intracellular cytoplasm and Dox could be selectively released upon the reaction of drug-conjugated SMNPs with the specific enzyme in the target cell lines. Longer incubation times (e.g., ≥ 72 h) of the drug-SMNP complexes in the targeted cell would lead to the red fluorescence accumulating more in the cell nuclei than in the cytoplasm (Figure S4 in the Supporting Information), demonstrating the dynamic process of drug release from the Dox-conjugated SMNP complexes in target HT-29 cells, in which enzyme-cleaved Dox was first released into the cytoplasm and then eventually diffused into the cell nuclei where Dox is known to react with topoisomerases to induce DNA damage and cytotoxicity.^[12] As a control, cellular imaging measurements were also conducted by incubating the cell lines with free Dox (Figure S5 in the Supporting Information). Upon incubation for two hours, a strong fluorescence was observed in the cell nuclei and relatively weak fluorescence in the cytoplasm, indicating different intracellular uptake between free Dox and drug-conjugated SMNPs. Compared with the Dox-SMNPs, the passive diffusion of

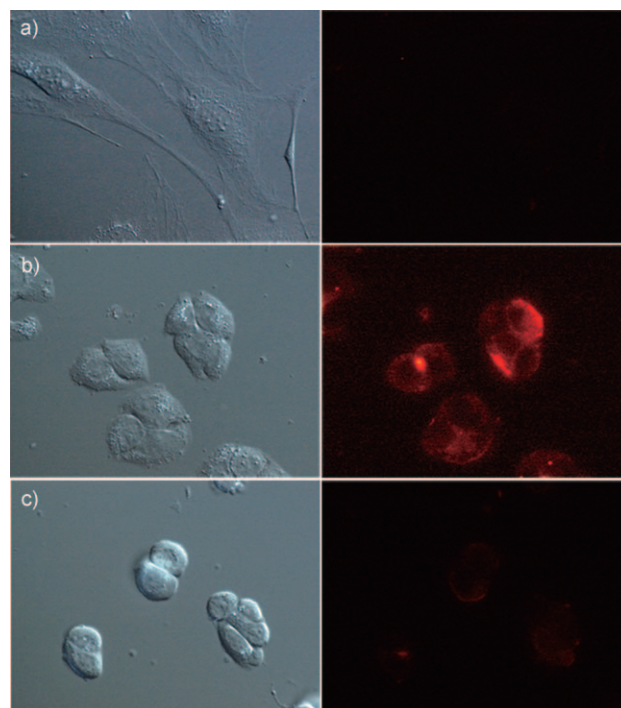


Figure 3. Confocal laser scanning microscopic images of a) NIH/3T3 cells incubated with 5.0 μ M Dox-SMNPs at 37 $^{\circ}$ C for 2 h, b) HT-29 cells incubated with 5.0 μ M Dox-SMNPs at 37 $^{\circ}$ C for 2 h, c) antipain hydrochloride inhibitor-pretreated HT-29 cells, incubated with 5.0 μ M Dox-SMNPs at 37 $^{\circ}$ C for 2 h ($\lambda_{\text{ex}}=535$ nm/50 nm, $\lambda_{\text{em}}=610$ nm/75 nm).

free Dox towards cell nuclei would lead to faster accumulation of the drug by intercalating into the DNA structure.^[4,12]

A similar cellular uptake of Dox-SMNPs was also evaluated by MRI spectroscopy. The Dox-SMNPs at various concentrations were incubated with HT-29 cells for two hours. After the cells were washed with phosphate buffered saline (PBS) and residual nanoparticles in solution were removed, the cells were evaluated by T2-weighted MRI. The signal intensity of the MRI decreased owing to the presence of the accumulation of SMNPs and the signal was also darker with increasing concentrations of Dox-SMNPs, as shown in Figure 4a. The intracellular uptake of SMNPs and Dox-SMNPs was further studied by inductively coupled plasma (ICP) (Figure 4b). ICP analysis of the concentrations of iron confirmed efficient cellular penetration of various concentrations of iron oxide nanoparticles and about 60% multifunctional nanoparticles were taken up by the HT-29 cells. A similar percentage of magnetic nanoparticle uptake was also found in the control NIH/3T3 cells (data not shown). These results clearly showed that Dox-SMNPs could easily enter into the cellular structures to work as an effective platform to monitor drug release in the different cell lines.

To evaluate the cytotoxicity and antitumor activity of Dox-SMNPs in living cells, cell viability was examined by standard 3-(4,5-dimethylthiazol-2-yl)-2,5-diphenyltetrazolium bromide (MTT) assay.^[12] In this typical study, both HT-29 and NIH/3T3 cancer cell lines were chosen to incubate with 5.0 μ M of Dox-SMNPs, free Dox, and SMNPs, respec-

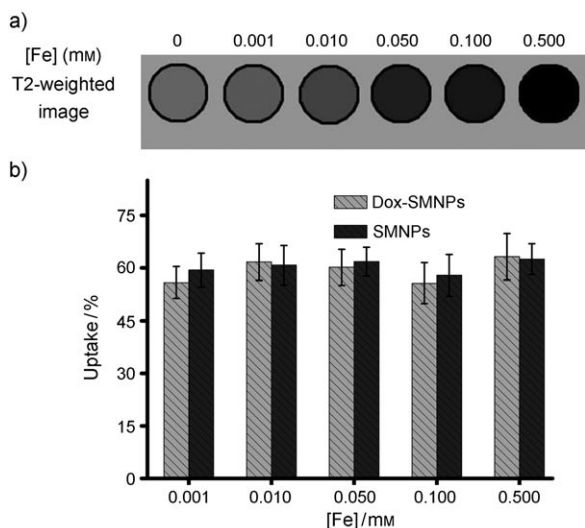


Figure 4. a) T2-weighted images of Dox-SMNPs in HT-29 cells. b) In vitro cellular uptake study of HT-29 cells after incubation for 2 h.

tively, at different time intervals. As shown in Figure 5, incubation of free particle SMNPs with HT-29 and NIH/3T3 cells did not lead to clear cytotoxicity to both of cells, indicating little toxicity caused by the as-prepared nanoparticles themselves. However, upon the incubation of Dox-SMNPs with HT-29 cells, significantly reduced cell viability could be

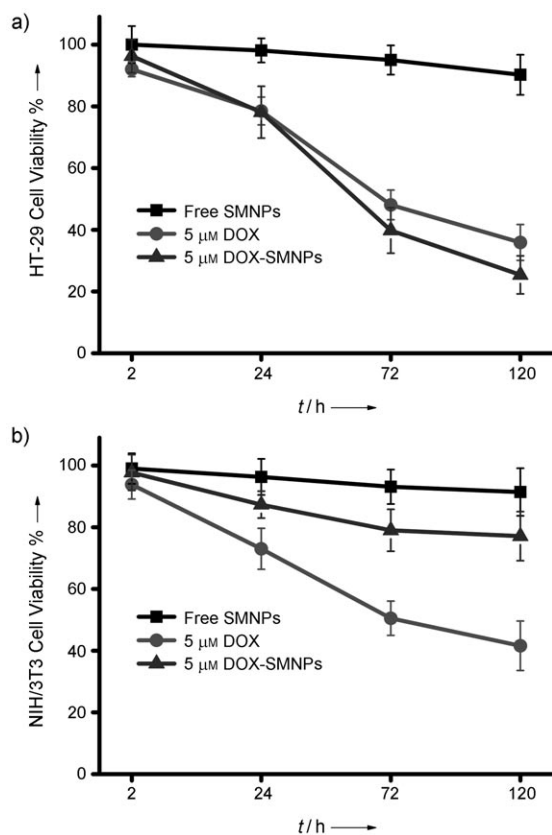


Figure 5. Cell viability assay of a) HT-29 and b) NIH/3T3 cells with free Dox (●), SMNPs (■), and Dox-SMNPs (▲).

observed. Compared with the HT-29 cells, limited changes in the cell viability were detected in NIH/3T3 cells. These results demonstrated that Dox-SMNPs could selectively interact with HT-29 cancerous cells, which had higher expression of cathepsin B enzymes and thus specifically released the anticancer drug into the target cells. As a commonly used anticancer drug, free Dox usually showed potent anticancer activity towards both HT-29 and NIH/3T3 cancer cell lines (Figure 5). But compared with free Dox, drug-conjugated SMNP complexes displayed different cytotoxic effects towards HT-29 and NIH/3T3 cancer cells. In HT-29 cells, free Dox had slightly higher cytotoxicity than Dox-SMNPs during short incubation times (e.g., 2 h) with the cells, most likely due to faster drug accumulation of free Dox inside the cell nuclei, as observed in cell imaging measurements. The comparable cytotoxicity between free Dox and Dox-conjugated SMNPs could be detected after a prolonged incubation time with HT-29 cells, the slightly higher cell viability of Dox-SMNPs could correspond to the efficient drug-delivery property of nanoparticles and their potent functions to circumvent the multidrug resistance effect, one situation in which free antitumor drugs could be pumped out from target cells thus inevitably decreased the therapeutic effect.^[13] In the control NIH/3T2 cell experiments, there was limited cytotoxicity of Dox-SMNPs observed for all time points of cell incubation, further confirming that Dox-SMNPs would selectively release the drug molecules and improve the drug activity significantly in the tumor cells with high cathepsin B expression levels, whereas the drug-conjugated nanoparticle complex exhibited lower cytotoxicity towards other cells without enzyme expression.

Conclusion

An enzyme-responsive multifunctional Dox-SMNPs complex has been synthesized by means of click chemistry. This stable and nontoxic SMNPs conjugated drug exhibited selective control of the release of antitumor drug molecules in living cells in which the specific enzyme has been highly expressed. This drug-loaded nanoparticle complex demonstrates promising properties for the real-time monitoring of intracellular drug release and tumor cell imaging by a combination of fluorescent imaging and MRI techniques. The multifunctional drug-coated hybrid nanoparticles provide the possibility for potential applications in tumor-targeted drug delivery and simultaneous diagnosis or detection of therapy intervention.

Experimental Section

Materials

All Fmoc-protected amino acids were from Bachem or GLChem. Other chemical reagents were purchased from Aldrich or Fluka. Cathepsin B and its inhibitor, antipain hydrochloride, were purchased from Sigma-Aldrich. The *N*-hydroxysuccinimide (NHS) ester of azido-dPEG₄ linker was purchased from Quanta Biosdesign. Commercially available reagents

were used without further purification. Anhydrous solvents for organic synthesis were purchased from Aldrich and stored over activated molecular sieves (4 Å). Thin-layer chromatography (TLC) was performed on precoated silica gel 60F₂₅₄ glass plates.

Instruments

¹H and ¹³C NMR spectra were recorded by using a Bruker 300 spectrometer. Mass spectra were measured on a Thermo Polaris Q instrument for EI measurements and a Thermo LCQ Deca XP MAX instrument for ESI measurements. HPLC analysis was performed on a reverse-phase column with a Shimadzu HPLC system. Analytical reverse-phase high-performance liquid chromatography (HPLC) was performed on Alltima C-18 column (250 × 3.0 mm) at a flow rate of 1.0 mL min⁻¹ and semi-preparative HPLC was performed on a similar C-18 column (250 × 10 mm) at a flow rate of 3 mL min⁻¹. UV absorption spectra were recorded in a 5 mm path quartz cell on a Beckman coulter DU800 spectrometer. Fluorescence emission spectra were performed on a Varian Cary eclipse fluorescence spectrophotometer. TEM images were collected on an FEI EM208S transmission electron microscope (Philips) operated at 120 kV. Fourier-transform infrared (FTIR) spectra were recorded on Shimadzu Irprestige-21 FTIR spectrophotometer. The size distribution of SMNPs was performed by using photon correlation spectroscopy (Brookhaven Instruments Corporation).

Preparation of H-Phe-Lys(Mtt)-OH (3)

Fmoc-Phe-OH (315 mg, 0.80 mmol) was dissolved in THF (5 mL) at 0°C to form a colorless solution. The solution was then treated with HOSu (96.5 mg, 0.83 mmol) and subsequently EDC (159.5 mg, 0.83 mmol) was added to the mixture and allowed to stir for 20 h. The generated product **1** was used in the next step of the synthesis without further purification. A stirred solution of Fmoc-lysine (Mtt)-OH (500 mg, 0.80 mmol) in DMF (2 mL) at room temperature was treated with piperidine/DMF (2 mL, 40%) for 2 h. The mixture was added to cold diethyl ether to obtain a precipitate, then centrifuged, and washed by diethyl ether (3 × 10 mL). A white precipitate, **2**, was collected and dried in vacuo. A mixture of **2** was dissolved in DMF (5 mL) and NEt₃ (115 μL) was slowly added to the mixture of solution. Compound **1** was slowly added to the mixture from the crude product in THF to form a colorless solution. The reaction mixture was allowed to continue stirring at room temperature for 22 h. The mixture was then dried by using a rotary evaporator and extracted with ethyl acetate (2 × 20 mL), then washed by water (2 × 20 mL) and brine (20 mL). The crude product was purified with flash chromatography with CH₂Cl₂/methanol (20:1) as the eluent to afford **3** as a white precipitate (290 mg, 70.1%). ¹H NMR (300 MHz; [D₆]DMSO, 25°C, TMS): δ = 1.30 (s, 2H), 1.45 (s, 2H), 1.60 (s, 2H), 1.95–2.05 (m, 2H), 2.21 (s, 3H), 2.80 (t, *J* = 12.9 Hz, 1H), 3.03 (d, *J* = 9.0 Hz, 1H), 4.05–4.33 (m, 5H), 7.01–7.38 (m, 23H), 7.74 (d, *J* = 8.2 Hz, 2H), 7.85 (d, *J* = 8.0 Hz, 2H), 8.08 ppm (brs, 1Hs); MS (70 eV): *m/z*: 772.06 [M+H]⁺.

Preparation of H-Phe-Lys(Mtt)-PABOH (5)

A solution of **3** (290 mg, 0.376 mmol) and PABOH (55.5 mg, 0.451 mmol) in anhydrous CH₂Cl₂ (8 mL) was treated at room temperature with EEDQ (139.5 mg, 0.564 mmol). The mixture was then stirred for 20 h. Finally, the mixture was concentrated at reduced pressure and washed with cold diethyl ether (3 × 5 mL). A white solid residue, **4** (329 mg, 99.0%), was formed and was used for the next step reaction without any further purification. MS: *m/z*: 876.85 [M+H]⁺.

A solution of **4** (329 mg, 0.376 mmol) in CH₂Cl₂ (8 mL) at room temperature was treated with diethylamine (16 mL). The mixture was allowed to stir at room temperature for 2 h. The solvent was evaporated and was purified with column chromatography MeOH/CH₂Cl₂ (20:1) to afford **5** as a white solid (198.9 mg, 81.1%). ¹H NMR (300 MHz, [D₆]DMSO, 25°C, TMS): δ = 1.21 (s, 2H), 1.36 (s, 2H), 1.90 (t, *J* = 7.0 Hz, 2H), 1.90–2.04 (m, 2H), 2.13–2.19 (m, 2H), 2.22 (s, 3H), 2.74 (dd, *J* = 9.0, 13.5 Hz, 1H), 3.21 (dd, *J* = 3.5, 13.5 Hz, 1H), 3.64 (dd, *J* = 3.6, 9.0 Hz, 1H), 4.57–4.61 (m, 3H), 7.03–7.05 (m, 2H), 7.12–7.45 (m, 21H), 7.95 (d, *J* = 8 Hz, 1H), 9.16 ppm (s, 1H); ¹³C NMR (75 MHz; [D₆]DMSO, 25°C, TMS): δ = 175.3, 170.0, 146.4, 143.2, 137.3, 137.2, 136.8, 135.7, 129.2, 128.8, 128.6, 128.5,

127.7, 127.6, 127.0, 126.1, 120.0, 70.6, 64.8, 60.4, 56.2, 53.8, 43.4, 40.8, 31.8, 30.7, 29.7, 23.5, 21.1, 20.9, 14.2 ppm; MS: *m/z*: 654.87 [M+H]⁺.

Preparation of Alkynyl-Phe-Lys(Mtt)-PABOH (6)

4-Pentynoic acid (500 mg, 5.09 mmol) was dissolved in THF (5 mL) at 0°C to form a colorless solution. The solution was then treated with HOSu (591.8 mg, 5.09 mmol), and subsequently, EDC (974.7 mg, 5.09 mmol) was added into the mixture and stirred for 22 h. The product was used directly for the next step synthesis without further purification. **5** (198.9 mg, 0.304 mmol) was dissolved in THF (5 mL) and the succinimide ester of 4-pentynoic acid (118.6 mg, 0.608 mmol) was added dropwise into the mixture cooled on an ice bath. The mixture was then treated with NEt₃ (50 μL) and stirred overnight. The mixture was then purified with flash chromatography with MeOH/CH₂Cl₂ (20:1) as the eluent with gradient to afford **6** as a yellow precipitate (156.3 mg, 70.0%). ¹H NMR (300 MHz, [D₆]DMSO, 25°C, TMS): δ = 1.24–1.69 (m, 6H), 1.96–2.05 (m, 2H), 2.24 (s, 3H), 2.41 (t, *J* = 3.0 Hz, 2H), 2.69–2.80 (m, 3H), 3.04 (d, *J* = 9.84 Hz, 1H), 4.38–4.57 (m, 4H), 7.05–7.53 (m, 21H), 8.11–8.16 (m, 2H), 9.94 ppm (s, 1H); ¹³C NMR (75 MHz; [D₆]DMSO, 25°C, TMS): δ = 171.6, 170.8, 170.7, 146.9, 143.7, 138.2, 138.0, 137.9, 135.4, 129.7, 128.8, 128.7, 128.4, 128.1, 127.4, 126.6, 126.4, 119.5, 84.1, 71.8, 71.7, 70.6, 63.0, 54.3, 54.0, 43.8, 38.3, 34.6, 32.6, 30.2, 24.3, 20.5, 14.8 ppm; MS: *m/z*: 734.97 [M+H]⁺.

Preparation of Alkynyl-Phe-Lys(Mtt)-PAB-PNP (7)

Compound **6** (156.3 mg, 0.213 mmol) was dissolved to CH₂Cl₂ (7 mL) and bis-PNP carbonate (325.1 mg, 1.07 mmol) was added to the mixture. Next, DIPEA (50 μL) was added into the reaction mixture and allowed to stir vigorously at room temperature for 2 days. After the starting material was consumed, as determined by TLC, the mixture was concentrated under reduced pressure and purified with flash chromatography with ethyl acetate and hexane (1:1) as the eluent. Compound **7** was obtained as a white precipitate (174.2 mg, 91.0%). ¹H NMR (300 MHz, [D₆]DMSO, 25°C, TMS): δ = 1.31–1.45 (m, 4H), 1.61–1.64 (m, 2H), 1.87 (s, 1H), 2.04–2.06 (m, 2H), 2.23 (s, 3H), 2.42–2.47 (m, 4H), 3.09 (d, *J* = 6.0 Hz, 2H), 4.68 (q, *J* = 6.0 Hz, 1H), 5.02 (dd, *J* = 6.0, 9.0 Hz, 1H), 5.29 (s, 2H), 7.01–7.45 (m, 23H), 7.63 (d, *J* = 8.0 Hz, 2H), 8.25 (d, *J* = 9.0 Hz, 2H), 9.18 ppm (s, 1H); ¹³C NMR (75 MHz; [D₆]DMSO, 25°C, TMS): δ = 171.5, 171.2, 170.1, 155.5, 152.5, 146.3, 145.4, 143.2, 138.6, 136.0, 135.7, 130.2, 129.7, 129.3, 128.6, 128.5, 128.4, 127.7, 126.1, 125.3, 121.8, 120.6, 82.8, 70.7, 70.6, 69.8, 54.4, 43.4, 39.0, 35.2, 30.8, 29.7, 23.7, 20.9, 15.0 ppm; MS: *m/z*: 899.99 [M+H]⁺.

Preparation of Dox–Peptide Substrate (9)

NEt₃ (100 μL) was added to a solution of **7** (174.2 mg, 0.193 mmol) and Dox-Cl (112.1 mg, 0.193 mmol) in dry DMF (8 mL). The solution was stirred at room temperature for 18 h and was extracted with ethyl acetate (3 × 10 mL), then washed with water (2 × 3 mL) and brine (1 × 3 mL). After concentrating the mixture under reduced pressure, mixture **8** was used for the next step without further purification. MS: *m/z*: 1304.07 [M+H]⁺.

The mixture of **8** was dissolved in CH₂Cl₂ (5 mL) and 1% TFA in CH₂Cl₂ (5 mL) was added dropwise into the suspension to form a clear red solution.^[6b] The solution was stirred at room temperature for 4 h and finally purified by HPLC. Compound **9** was obtained after lyophilization as a red solid product (81.1 mg, 40.7%). MS: *m/z*: 1048.26 [M+H]⁺.

Preparation of Colloidal Iron Oxide Nanoparticles

The magnetic iron oxide nanoparticles were prepared as described previously.^[8b] Typically, magnetic nanoparticles were prepared based on the chemical co-precipitation of Fe²⁺ and Fe³⁺ by adding a concentrated base, sodium hydroxide (10 M), to the mixture of iron salts with a molar ratio (FeCl₂/FeCl₃) of 1:2. The mixture was stirred vigorously for 1 h at room temperature and was further heated to 90°C for another 1 h. Trisodium citrate solution (0.3 M, 200 mL) was added to the mixture and heating was continued for another 30 min. The mixture was then cooled to room temperature and the magnetic particles were precipitated with acetone and the supernatant was decanted with a magnet. Water was then

added to redisperse the magnetic particles, which were and sent for dialysis for one week.

Preparation of SMNPs

SMNPs were synthesized by the Stöber method. The coating of the iron oxide with silica was carried out in ethanol and Milli-Q water in a ratio of (4:1). Iron oxide in Milli-Q water (1.5 wt %, 2 mL) was suspended in ethanol (160 mL) and Milli-Q water (40 mL) and followed by adding aqueous ammonia (25 %, 5 mL). This suspension was then homogenized by ultrasonic vibration in a water bath for 15 min. Next, tetraethylorthosilicate/3-(aminopropyl)triethoxysilane (10:1; 500 μ L) was added dropwise to the mixture under continuous mechanical stirring. After reaction for 12 h, the mixture was washed thoroughly with ethanol and dried in vacuo to obtain the desired iron oxide coated with silica (46.0 mg). The surface amino groups were quantified at 1.5 mmol g⁻¹ by the ninhydrin test.^[14]

Preparation of Azido-dPEG₄-Functionalized SMNPs

The azido-dPEG₄-functionalized, silica-coated iron oxide nanoparticles (azido-dPEG₄-functionalized SMNPs) were synthesized by dissolving the SMNPs (46.0 mg) in DMF (2 mL). Next, azido-dPEG₄-NHS ester (0.14 mmol) in DMF was added dropwise into the suspension. Under continuous stirring, NEt₃ (20 μ L) was added to the mixture and stirred overnight at room temperature. The suspension was washed with ethanol 5 times and centrifuged at 1 \times 10⁴ rpm to obtain the supernatant. Azido-dPEG₄-functionalized SMNPs were analyzed by FTIR (Figure S6 in the Supporting Information).

Preparation of Dox-SMNPs by Click Chemistry

The azido-dPEG₄-functionalized SMNPs were clicked with acetylene-functionalized Dox-peptide substrate by dissolving the azido-dPEG₄ SMNPs into water/*tert*-butanol (4 mL, 1:1). Then Dox-peptide substrate (3.1 mg, 0.003 mmol) was added to the mixture. Subsequently, ascorbic acid (200 mM, 100 μ L) and copper(II) sulfate (200 mM, 50 μ L) were added. The mixture was allowed to stir for 1 day at room temperature and was washed with deionized water (5 \times) and centrifuged at 1 \times 10⁴ rpm to obtain the final product Dox-SMNPs; the supernatant and washed solution were collected. The loading amount of Dox-peptide substrate was calculated by the difference in UV absorbance spectra ($\epsilon_{495} = 8030 \text{ cm}^{-1} \text{ M}^{-1}$).^[4b,c,5a,15]

Enzymatic Assays Enzymatic Activity for Dox-Peptide Substrates

The stock solution of cathepsin B was dissolved in 25 mM of acetate buffer/1 mM ethylenediaminetetraacetic acid (EDTA) (pH 5.00). Dox-peptide substrate was also dissolved in 25 mM of acetate buffer/1 mM EDTA (pH 5.00) (0.5 % DMSO). Cathepsin B (10 μ L) was first activated in 60 mM DL-dithiothreitol (DTT)/15 mM EDTA (5 μ L) for 30 min under room temperature then incubated with Dox-peptide substrate (85 μ L) for different time intervals; the final concentration of Dox-peptide substrate and cathepsin B were 100 μ M and 33 nM, respectively. The enzyme reaction was analyzed by HPLC at a wavelength of 485 nm (Figure S1 in the Supporting Information).

Enzymatic Activity for Dox-SMNPs

The stock solution of cathepsin B was dissolved in 25 mM acetate buffer/1 mM EDTA at pH 5.00. Dox-SMNPs was similarly dissolved in 25 mM acetate buffer/1 mM EDTA at pH 5.00. Cathepsin B (10 μ L) was first activated in 60 mM DTT/15 mM EDTA (5 μ L) for 30 min at room temperature then incubated with Dox-SMNPs (85 μ L; concentration: 0–100 μ M) at different time intervals (0–6 h). The fluorescent enhancement was monitored by using a fluorescence spectrophotometer with an excitation wavelength of 485 nm (Figure S7 in the Supporting Information).

In Vitro Enzyme Inhibition Assays

The enzyme cathepsin B was pretreated with antipain hydrochloride inhibitor (100 μ M) for 2 h at 37 °C, then incubated with Dox-SMNPs (final concentration 100 μ M) for another 2 h for fluorescent measurement.

Living-Cell Assays

The HT-29 cell line was bought from the American-type culture collection (ATCC Cat No: HTB-38) and maintained in McCoy's 5a medium (ATCC, Manassas VA) containing 10 % fetal bovine serum (FBS) (Invitrogen, Burlington, Canada). The HT-29 cell lines were seeded at a density of 2 \times 10⁵ in a 35 mm diameter μ -dish plastic bottom (ibidi GmbH, Germany) and cultured for 2 days in McCoy's 5a medium with L-glutamine (ATCC). The control NIH/3T3 cell line was also bought from ATCC (cat. no.: CRL-2795) and cultured with the same protocol as HT-29, except the medium used was DMEM.

Cell-Viability Measurements^[12]

HT-29 was seeded with a cell density of 1 \times 10⁴ cells per well in 96-well plates in McCoy's 5a medium. The cells were cultured at 37 °C for 2 days. Dox-SMNPs (5 μ M), Dox (5 μ M), and free SMNPs were incubated in McCoy's 5a medium for 0–120 h. At the end of the experiment, the cells were supplied with fresh McCoy's 5a medium and MTT solution (1.0 mg mL⁻¹) in medium was then added. The plates were incubated for 4 h at 37 °C, then the MTT-containing medium was removed and DMSO (100 μ L) was added to dissolve the formazan crystals formed by the living cells. Absorbance was measured at 560 nm by using a Bio-Tek EL-311 microplate reader. The cell viability was calculated according Equation (1):

$$\text{cell viability (\%)} = \frac{(\text{OD}_{560}(\text{sample}) - \text{OD}_{560}(0))}{(\text{OD}_{560}(\text{control}) - \text{OD}_{560}(0))} \times 100\% \quad (1)$$

in which OD₅₆₀(sample) represents the measurement from the wells treated with Dox-SMNPs, Dox, and SMNPs and OD₅₆₀(control) represents the measurement from the wells treated with 25 mM of acetate buffer/1 mM EDTA at pH 5.00 in medium. OD₅₆₀(0) represents the blank absorbance. Control NIH/3T3 cell lines were performed by using the same protocol except with a different culture medium, DMEM.

Cell Imaging

The living HT-29 and NIH/3T3 cells were cultured in 35 mm plastic-bottomed μ -dishes for 2 days and then the cells were washed twice with McCoy's 5a medium and DMEM. The cells were treated with Dox-SMNPs (5 μ M) in McCoy's 5a medium (HT-29) and DMEM (NIH/3T3) and incubated for 0–96 h at 37 °C. After the cells were washed twice with Hank's balanced salt solution (HBSS), cell imaging was conducted under a confocal fluorescence microscope (Nikon, Eclipse TE2000-E) with an excitation filter (535 nm/50 nm) and an emission filter (610/75 nm) (Figure S3 in the Supporting Information).

Cell Inhibition Assay

The live HT-29 cell lines were washed twice with McCoy's 5a medium and pretreated separately with 5 μ M antipain hydrochloride in McCoy's 5a medium for the required time points (0.5 or 2 h) at 37 °C. Dox-SMNPs were then added with a final concentration of 5 μ M and incubated for another 0.5 or 2 h. The cells were washed twice with HBSS for living-cell imaging and cell lysate fluorescent measurements.

For the cell lysate fluorescent measurements, typically, the Dox-SMNP-incubated HT-29 cell lines (in the absence and presence of enzyme inhibitor) were treated with trypsin and washed three times with HBSS. Then, the mixture underwent a freeze-thaw cycle (water bath, 37 °C) five times. The supernatant was then sonicated at 4 °C for 10 min and subsequently centrifuged at 10000 rpm for 10 min for fluorescent detection at 590 nm.

MRI In Vitro Cellular-Uptake Study: Phantom Study

SMNPs were suspended in 0.5 % agarose gel in 300 μ L polymerase chain reaction (PCR) tubes. The tubes were embedded in a homemade tank, which was designed to fit the MRI coil and was filled with 0.5 % agarose gel. T2-weighted MRI images were acquired on a GE 7.0 T small-animal MRI system with the following parameters: TR 3000 ms; TE 20, 40, 60, 80, 100, 120 ms; flip angle 30°; FOV 6 \times 6, 256 \times 256 matrix; slice thickness 1 mm.

The different cells were cultured in 10 cm culture dishes in an incubator. When the cells reached 90% confluency, two kinds of particles, SMNPs and Dox-SMNPs, with different iron concentrations^[5a] in culture medium without FBS were added and incubated for 2 h at 37°C in an incubator. After being washed twice with PBS, the cells were collected and suspended in 150 µL PBS tubes and were sonicated for 2 h. The sonicated cell lysate containing particles were suspended in 0.5% agarose gel in 300 µL PCR tubes and the phantom studies were conducted as described above. After the cell phantom study, the cell lysates were dissolved in nitric acid and heated at 90°C for 2 h. After heating, cell lysates were diluted in distilled water and added into sample tubes. The iron concentration was measured by inductively coupled plasma (ICP) spectrometry. The cell uptake of the particles was calculated based on the input iron amount and the amount remaining in the cells.

Acknowledgements

We gratefully acknowledge Start-Up Grant (SUG), RG64/10, and A*Star BMRC (07/1/22/19/534) grants from Nanyang Technological University, Singapore, and grants NIH1R41A137960 and NCIP50A119367 from National Institute of Health (NIH), USA.

- [1] a) G. Schmid, *Nanoparticles: From Theory to Applications*; Wiley-VCH, Weinheim, **2004**; b) C. M. Niemeyer, C. A. Mirkin, *Nanobiotechnology: Concepts, Applications and Perspectives*, Wiley-VCH, Weinheim, **2004**; c) N. L. Rosi, C. A. Mirkin, *Chem. Rev.* **2005**, *105*, 1547–1562; d) J. Xie, J. Huang, X. Li, S. Sun, X. Chen, *Curr. Med. Chem.* **2009**, *16*, 1278–1294; e) M. Zhou, R. Zhang, M. Huang, W. Lu, S. Song, M. P. Melancon, M. Tian, D. Liang, C. Li, *J. Am. Chem. Soc.* **2010**, *132*, 15351–15358; f) G. Zhang, Z. Yang, W. Lu, R. Zhang, Q. Huang, M. Tian, L. Li, D. Liang, C. Li, *Biomaterials* **2009**, *30*, 1928–1936; g) R. R. Liu, R. Liew, J. Zhou, B. G. Xing, *Angew. Chem.* **2007**, *119*, 8955–8959; *Angew. Chem. Int. Ed.* **2007**, *46*, 8799–8803; h) T. T. Jiang, R. R. Liu, X. F. Huang, H. J. Feng, W. L. Teo, B. G. Xing, *Chem. Commun.* **2009**, 1972–1974; i) H. Feng, Y. M. Yang, Y. You, G. Li, J. Guo, T. Yu, Z. X. Shen, T. Wu, B. G. Xing, *Chem. Commun.* **2009**, 1984–1986.
- [2] a) C. C. Berry, A. S. G. Curtis, *J. Phys. D* **2003**, *36*, R198–R206; b) C. Corot, P. Robert, J. M. Idee, M. Port, *Adv. Drug Delivery Rev.* **2006**, *58*, 1471–1504.
- [3] a) J. H. Park, G. Maltzahn, E. Ruoslahti, S. N. Bhatia, M. J. Sailor, *Angew. Chem.* **2008**, *120*, 7394–7398; *Angew. Chem. Int. Ed.* **2008**, *47*, 7284–7288; b) C. Lai, Y. Wang, C. Lai, M. Yang, C. Chen, P. Chou, C. Chan, Y. Chi, Y. Chen, J. Hsiao, *Small* **2008**, *4*, 218–224; c) J. H. Gao, G. L. Liang, J. Chang, Y. Pan, Y. Kuang, F. Zhao, B. Zhang, X. X. Zhang, E. X. Wu, B. Xu, *J. Am. Chem. Soc.* **2008**, *130*, 11828–11833; d) R. Weissleder, K. Kelly, E. Sun, T. Shtatland, L. Josephson, *Nat. Biotechnol.* **2005**, *23*, 1418–1423; e) C. Kaittanis, S. Santra, J. M. Perez, *J. Am. Chem. Soc.* **2009**, *131*, 12780–12791; f) H. Lee, M. K. Yu, S. Park, S. Moon, J. J. Min, Y. Y. Jeong, H. Kang, S. Y. Jon, *J. Am. Chem. Soc.* **2007**, *129*, 12739–12745; g) J. H. Gao, H. W. Gu, B. Xu, *Acc. Chem. Res.* **2009**, *42*, 1097–1107; h) A. T. Kell, G. Stewart, S. Ryan, R. Peytavi, M. Boissinot, A. Huletsky, M. G. Bergeron, B. Simard, *ACS Nano* **2008**, *2*, 1777–1788; i) J. H. Lee, M. V. Yigit, D. Mazumdar, Y. Lu, *Bioconjugate Chem.* **2008**, *19*, 412–417; j) M. V. Yigit, D. Mazumdar, Y. Lu, *Adv. Drug Delivery Rev.* **2010**, *62*, 592–605; k) J. Xie, K. Chen, H. Y. Lee, C. J. Xu, A. R. Hsu, S. Peng, X. Chen, S. Sun, *J. Am. Chem. Soc.* **2008**, *130*, 7542–7543; l) T. K. Jain, J. Richey, M. Strand, D. L. Leslie-Pelecky, C. A. Flask, *Biomaterials* **2008**, *29*, 4012–4021.
- [4] a) J. R. Hwu, Y. S. Lin, T. Josephraj, M. H. Hsu, F. Y. Cheng, C. S. Yeh, W. C. Su, D. B. Shieh, *J. Am. Chem. Soc.* **2009**, *131*, 66–68; b) J. E. Lee, N. Lee, H. Kim, J. Kim, J. Kim, S. H. Choi, J. H. Kim, T. Kim, I. C. Song, S. P. Park, W. K. Moon, T. Hyeon, *J. Am. Chem. Soc.* **2010**, *132*, 552–557; c) L. Zhu, T. Ikoma, N. Hanagata, S. Kaskel, *Small* **2010**, *6*, 471–478; d) F. Dilnawaz, A. Singh, C. Mohanty, S. K. Sahoo, *Biomaterials* **2010**, *31*, 3694–3706; e) S. Guo, D. Li, L. Zhang, J. Li, E. Wang, *Biomaterials* **2009**, *30*, 1881–1889; f) B. Wang, C. J. Xu, J. Xie, Z. Y. Yang, S. H. Sun, *J. Am. Chem. Soc.* **2008**, *130*, 14436–14437.
- [5] a) M. K. Yu, Y. Y. Jeong, J. Park, S. Park, J. W. Kim, J. J. Min, K. Kim, S. Jon, *Angew. Chem.* **2008**, *120*, 5442–5445; *Angew. Chem. Int. Ed.* **2008**, *47*, 5362–5365; b) J. M. Yang, C. H. Lee, H. J. Ko, J. S. Suh, H. G. Yoon, K. Y. Lee, Y. M. Huh, S. J. Haam, *Angew. Chem.* **2007**, *119*, 8992–8995; *Angew. Chem. Int. Ed.* **2007**, *46*, 8836–8839; c) G. von Maltzahn, Y. Ren, J. H. Park, D. H. Min, V. R. Kotamraju, J. Jayakumar, V. Fogal, M. J. Sailor, E. Ruoslahti, S. N. Bhatia, *Bioconjugate Chem.* **2008**, *19*, 1570–1578.
- [6] a) F. Lecaille, J. Kaleta, D. Bromme, *Chem. Rev.* **2002**, *102*, 4459–4488; b) K. A. Ajaj, M. L. Binossek, F. Kratz, *Bioconjugate Chem.* **2009**, *20*, 390–396; c) K. Miller, R. Erez, E. Segal, D. Shabat, R. S-Fainaro, *Angew. Chem.* **2009**, *121*, 2993–2998; *Angew. Chem. Int. Ed.* **2009**, *48*, 2949–2954.
- [7] a) S. Fuchs, H. Otto, S. Jehle, P. Henklein, A. D. Schluter, *Chem. Commun.* **2005**, 1830–1832; b) S. Krueger, T. Kalinski, H. Wolf, U. Kellner, A. Roessner, *Cancer Lett.* **2005**, *223*, 313–322; c) M. Calderón, R. Graeser, F. Kratz, R. Haag, *Bioorg. Med. Chem. Lett.* **2009**, *19*, 3725–3728; d) M. Funovics, R. Weissleder, C. Tung, *Anal. Bioanal. Chem.* **2003**, *377*, 956–961.
- [8] a) Y. Lu, Y. Yin, B. T. Mayers, Y. Xia, *Nano Lett.* **2002**, *2*, 183–186; b) G. Li, D. L. Zeng, L. Wang, B. Zong, K. G. Neoh, E. T. Kang, *Macromolecules* **2009**, *42*, 8561–8565.
- [9] a) F. H. Chen, Q. Chao, J. Z. Ni, *Nanotechnology* **2008**, *19*, 165103; b) S. Santra, R. Tapeç, N. Theodoropoulou, J. Dobson, A. Hebard, W. H. Tan, *Langmuir* **2001**, *17*, 2900–2906.
- [10] J. D. Gibson, B. P. Khanal, E. R. Zubarev, *J. Am. Chem. Soc.* **2007**, *129*, 11653–11661.
- [11] F. Lu, S. Wu, Y. Hung, C. Mou, *Small* **2009**, *5*, 1408–1413.
- [12] a) F. Zunino, G. Capranico, *Anti-Cancer Drug Des.* **1990**, *5*, 307–317; b) J. Y. Kim, J. E. Lee, S. H. Lee, J. H. Yu, J. H. Lee, T. G. Park, T. J. Hyeon, *Adv. Mater.* **2008**, *20*, 478–483; c) I. B. Kim, H. Shin, A. J. Garcia, U. H. F. Bunz, *Bioconjugate Chem.* **2007**, *18*, 815–820; d) H. S. Yoo, K. H. Lee, J. E. Oh, T. G. Park, *J. Controlled Release* **2000**, *68*, 419–431; e) S. D. Brown, P. Nativo, J. Smith, D. Stirrington, P. R. Edwards, B. Venugopal, D. J. Flint, J. A. Plumb, D. Graham, N. J. Wheate, *J. Am. Chem. Soc.* **2010**, *132*, 4678–4684.
- [13] a) A. C. de Verdiere, C. Dubernet, F. Nemat, M. F. Poupon, F. Puisieux, P. Couvreur, *Cancer Chemother. Pharmacol.* **1994**, *33*, 504–508; b) D. Peer, J. M. Karp, S. Hong, O. C. Farokhzad, R. Margalit, R. Langer, *Nat. Nanotechnol.* **2007**, *2*, 751–760.
- [14] a) M. M. Leane, R. Nankervis, A. Smith, L. Illum, *Int. J. Pharm.* **2004**, *271*, 241–249; b) Y. Zhao, B. G. Trewyn, I. I. Slowing, V. S. Lin, *J. Am. Chem. Soc.* **2009**, *131*, 8398–8400.
- [15] G. M. Dubowchik, R. A. Firestone, L. Padilla, D. Willner, S. J. Hofstead, K. Mosure, J. O. Knipe, S. J. Lasch, P. A. Trail, *Bioconjugate Chem.* **2002**, *13*, 855–869.

Received: December 17, 2010

Published online: May 4, 2011